

Matrix-weighted networks for modeling multidimensional dynamics

Yu Tian,¹ Sadamori Kojaku,² Hiroki Sayama,^{2,3} and Renaud Lambiotte⁴

¹*Nordita, Stockholm University and KTH Royal Institute of Technology, Sweden*

²*School of Systems Science and Industrial Engineering, Binghamton University, USA*

³*Waseda University, Japan*

⁴*University of Oxford, UK*

Networks are powerful tools for modeling interactions in complex systems. While traditional networks use scalar edge weights, many real-world systems involve multidimensional interactions. For example, in social networks, individuals often have multiple interconnected opinions that can affect different opinions of other individuals, which can be better characterized by matrices. We propose a novel, general framework for modeling such multidimensional interacting dynamics: matrix-weighted networks (MWNs). We present the mathematical foundations of MWNs and examine consensus dynamics and random walks within this context. Our results reveal that the coherence of MWNs gives rise to non-trivial steady states that generalize the notions of communities and structural balance in traditional networks.

Networks have emerged as a powerful model for studying interacting systems across a wide range of disciplines, enhancing our understanding of complex systems such as the human brain, the Internet, and human societies [1]. Networks are constructed from pairwise interactions between entities which, combined together, allow for signals to propagate in connected systems. Much effort has been made to understand the intricate interplay between dynamical systems on networks and underlying network structure [2–5] with two main foci: examining the network properties that influence dynamics on networks, and utilizing dynamical processes to extract valuable information about underlying network structure. For example, modular structure in networks can effectively simplify the description of dynamical systems [5, 6] and, in the presence of negative links, structural balance can help separate distinct dynamical behaviors [7–9].

How to characterize pairwise interaction is a key modeling decision that significantly impacts the analysis of network dynamics. Widespread choices include binary values indicating the presence or absence of an edge between two nodes, a positive real number to indicate connection strength, and a real value whose sign represents consolidation or contradiction [1]. Recent studies have expanded the concept of edge weights to complex values [10, 11] to represent the “state” of connections.

Recent years have also witnessed a movement towards multi-dimensional characterizations of node states and their interactions in various network models, such as multiplex networks and multi-layer networks [12–15]. In general, higher-dimensional variables and multi-dimensional interactions naturally arise in a variety of applications [16–20]. For example, in image processing, each image necessarily lies in a higher-dimensional space, and it has been shown that more robust results can be obtained by considering the transformations in higher dimensions [18]. In social systems, it is natural that more than one statement is propagating through the networks, where the belief in one affects the belief in others [20–26].

However, the details of such nontrivial multidimensional interactions *between nodes* are not fully reflected in traditional network models. Edges in existing models with multidimensional node states are typically assumed to simply transmit a vector from one node to another, and/or to compare two vector states and react according to their distances, e.g. [20]. These simple assumptions would be too limited to capturing more complex multidimensional interactions identified in various real-world network systems. This observation has led us to study multidimensional *interaction* models. Models for multidimensional interactions have been previously studied, particularly in opinion dynamics [27, 28]. In these models, agents possess opinion vectors on various topics that can change in nontrivial ways through communication, depending on how agents interpret their neighbors’ opinions. While these models have found applications in machine learning [29–32], their translation to physical systems and complex network dynamics remains largely unexplored, leaving opportunities to enhance our understanding of multifaceted interactions in complex networks.

In this article, we introduce a framework specifically designed for multidimensional interactions on networks, *matrix-weighted networks* (MWNs). This is a generalization of conventional scalar- or complex-weighted network models, in which one can represent a linear transformation of state vectors between a pair of nodes connected by an edge. In most general settings, the weights can be any matrices of any size or shape (even rectangular ones may be allowed if the dimensions of node states differ from node to node) and self-loops are permitted, where not only multidimensional interactions of node states but also any network with any partitions can be analyzed from the angle of MWNs. In this paper, we start with the cases of square matrix weights and directed edge reciprocity which, as we argue, can be seen as the generalization of classical undirected networks to the matrix-weighted setting. More specifically, we consider the cases when

edges characterize reciprocal interactions, where the effect of one characteristic dimension of node states on another dimension from one node to another is the same as the one when the orders of both nodes and dimensions are reversed. This choice lends itself to the study of orthogonal matrices, where isometries are defined on each edge. We start by providing mathematical foundations for MWNs, and then characterize the dynamical behavior through two key dynamics, consensus dynamics and random walks that are reformulated with this framework, both theoretically and numerically. Our main results concern the definition of the coherence of MWNs, which determines the existence of non-trivial steady states for the dynamics and is associated with large-scale patterns generalizing the notions of communities and structural balance. Finally, we discuss opportunities for future research and connections with existing network models. The code and documentation to reproduce all numerical results can be found at our GitHub repository [33].

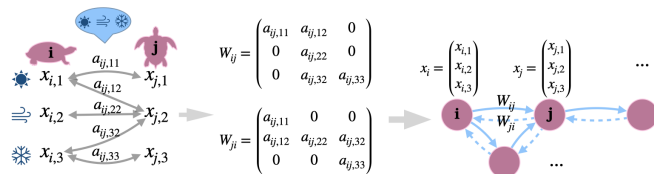


FIG. 1: Illustration of a MWN, where each node is equipped with 3 state variables. In an opinion dynamics setting, each variable can be interpreted as an opinion on a specific topic. Here, we illustrate how the state vector of node v_i affects the state vector of v_j and vice versa.

Matrix-weighted networks (MWNs). We consider networks in the form of weighted graphs $G = (V, E, \mathcal{W})$, being connected and directed, where $V = \{v_1, v_2, \dots, v_n\}$ is the node set and $E \subset V \times V$ is the edge set. We use a matrix $\mathbf{W}_{ij} \in \mathbb{R}^{n_d \times n_d}$ to characterise the relationship between nodes v_i and v_j , where n_d is the characteristic dimension. \mathbf{W}_{ij} is the all-zero matrix if and only if there is no directed edge from v_i to v_j . Otherwise, the matrix encodes how a n_d -dimensional signal on node v_j impacts the signal on node v_i . See Fig. 1 for an example. We define the $(n \ n_d) \times (n \ n_d)$ supra-weight matrix \mathcal{W} to have block structure, with the i, j block being \mathbf{W}_{ij} , the matrix weight between nodes v_i and v_j . Furthermore, we decompose each matrix weight into two parts, one accounting for the magnitude $w_{ij} = \|\mathbf{W}_{ij}\|_2$, and the other for the transformation \mathbf{R}_{ij} with $\|\mathbf{R}_{ij}\|_2 = 1$ (for $w_{ij} > 0$), such that $\mathbf{W}_{ij} = w_{ij}\mathbf{R}_{ij}$. In this paper, we assume that $\mathbf{W}_{ij} = \mathbf{W}_{ji}^T$, i.e., the interaction between the same pair of dimensions is reciprocal between the same pair of nodes. Then we have $w_{ij} = w_{ji}$, $\mathbf{R}_{ij} = \mathbf{R}_{ji}^T$, and finally, $\mathcal{W}^T = \mathcal{W}$. This choice ensures that the eigenvalues of \mathcal{W} are real numbers, and can be understood as an extension of undirected networks to the matrix-weighted

setting.

We define the degree (or strength) of a node v_i as the sum of the matrix norm of edges incident on this node,

$$d_i = \sum_j \|\mathbf{W}_{ij}\|_2 = \sum_j w_{ij},$$

and the supra-degree matrix as

$$\mathcal{D} = \mathbf{D} \otimes \mathbf{I},$$

where \mathbf{D} is the diagonal matrix with $\mathbf{d} = (d_i)$ on its diagonal, \mathbf{I} is the identity matrix in $\mathbb{R}^{n_d \times n_d}$, and \otimes denotes Kronecker product. We define the supra-Laplacian matrix as

$$\mathcal{L} = \mathcal{D} - \mathcal{W}.$$

We note that there are other types of Laplacian considered in the multidimensional setting, such as the one based on node-edge interactions [28], but ours is more consistent with existing network science models, thus more appropriate to adapt network-based methods. If we consider a vector $\mathbf{x} = (\mathbf{x}_1; \mathbf{x}_2; \dots; \mathbf{x}_n)$ with $\mathbf{x}_i \in \mathbb{R}^{n_d}$ for each i , then we can write

$$\mathbf{x}^T \mathcal{L} \mathbf{x} = \sum_{(v_i, v_j), (v_j, v_i) \in E} w_{ij} \|\mathbf{x}_i - \mathbf{R}_{ij} \mathbf{x}_j\|_2^2 \geq 0. \quad (1)$$

Hence, the supra-Laplacian matrix maintains the property of the matrix Laplacian to be positive semi-definite. We then define the supra-random-walk Laplacian matrix as

$$\mathcal{L}_{rw} = \mathcal{I} - \mathcal{P},$$

where $\mathcal{I} \in \mathbb{R}^{nn_d \times nn_d}$ is the identity matrix and $\mathcal{P} = \mathcal{D}^{-1} \mathcal{W}$ is the supra-transition matrix. Clearly, if $n_d = 1$, we retrieve the classic definitions. We will show later that the supra-Laplacian matrix and the supra-random-walk Laplacian matrix are closely related to the consensus dynamics and the random walks, respectively, in the multi-dimensional case.

Coherence. We define the *transformation* of a directed path P with composing edges e_1, e_2, \dots, e_k as

$$\mathbf{R}(P) = \mathbf{R}(e_1)\mathbf{R}(e_2)\dots\mathbf{R}(e_k),$$

where $\mathbf{R}(e)$ returns the transformation of edge e . The transformation of a directed cycle is defined similarly. This notion is essential to understand how signals propagate along walks in the graph. As we will see, in certain graphs, different walks to the same node will be associated to different linear transformations, and hence to conflicting signals, while in other graphs, walks to the same node will always result in the same linear transformation and thus to reinforcement akin to resonance. The presence or absence of conflicts along the walks is de-

scribed by the notion of *coherence*, which we define now, and determines the asymptotic of the dynamics studied in this paper.

We define a matrix-weighted network G to be *coherent* if and only if the transformation of every directed cycle is \mathbf{I} . An immediate consequence for a graph to be coherent is that all matrix weights are orthogonal under the assumptions adopted in this paper, since for each edge $(v_i, v_j) \in E$, we also have $(v_j, v_i) \in E$, and for the directed cycle of the two reciprocal edges to have transformation \mathbf{I} , we have $\mathbf{R}_{ij}\mathbf{R}_{ji} = \mathbf{R}_{ij}\mathbf{R}_{ij}^T = \mathbf{I}$. Note that this definition, which naturally describes the geometrical problems considered in this paper, is strict, hence we also quantify the *level of coherence* by how far the network is from being coherent, e.g., through the portion of cycles that do not have \mathbf{I} as the transformation. Furthermore, the notion can also be relaxed in other contexts, as we discuss in Supplemental Material (SM).

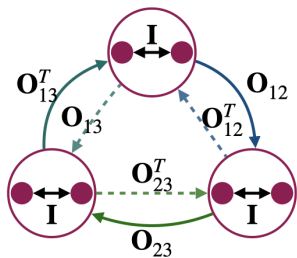


FIG. 2: Example of the block structure of a coherent MWN, where the label indicates the orthogonal matrix weights and $\mathbf{O}_{13} = \mathbf{O}_{12}\mathbf{O}_{23}$

The notion of coherence also characterizes particular block structures in the MWN. Suppose there is a partition of G such that (i) any edges within each block have transformation \mathbf{I} , and (ii) any edges between the same pair of blocks have the same transformation, thus we can consider each block as a super node; see Fig. 2. Then if (iii) any directed cycles of such super nodes have transformation \mathbf{I} , we can immediately see that the MWN is coherent, since any directed cycles in the network, apart from edges inside each block, form directed cycles of the super nodes (if not empty). We also show that such block structure always exists in coherent MWN in SM, hence uniquely defining the coherence.

With the characteristic block structure, we can connect all coherent networks with the *identity-transformed MWN* where the transformation of each edge is \mathbf{I} . The identity-transformed MWN is a typical coherent MWN, and has supra-Laplacian

$$\bar{\mathcal{L}} = \bar{\mathbf{L}} \otimes \mathbf{I},$$

where $\bar{\mathbf{L}} = \mathbf{D} - \bar{\mathbf{W}}$ and $\bar{\mathbf{W}} = (w_{ij})$ only maintains the magnitude of each edge weight, thus $\bar{\mathbf{L}}$ is the classic graph Laplacian for positive scalar weights. For a

coherent MWN, we encode its intrinsic block structure into a block diagonal matrix, \mathcal{S} : its i -th block on the diagonal returns the transformation of any directed paths from nodes in the first block to the block that node v_i belongs to. Then,

$$\mathcal{L} = \mathcal{S}^T \bar{\mathcal{L}} \mathcal{S}.$$

Hence, the supra-Laplacian also has eigenvalue 0, and the associated eigenvectors span the subspace

$$\mathbf{X} = \mathcal{S}^T (\mathbf{1} \otimes \mathbf{I}).$$

We also show that the existence of 0 as an eigenvalue always leads to coherence in SM, hence also intrinsic to the coherent MWN.

Consensus dynamics. Consensus has been one of the most important dynamics on networks, with various applications [34–37]. Note that matrix relationship (or *logic constraints*) has been considered in the belief formation of multiple statements [20], but we incorporate transformation in the propagation process, as we will see later. Now, let us endow each node with a vector state variable, $\mathbf{y}_i \in \mathbb{R}^{n_d}$, and the interdependence between the dimensions are encoded in the matrix weights $\{\mathbf{W}_{ij}\}$. The *consensus dynamics* can then be defined as

$$\dot{\mathbf{y}}_i = \sum_j w_{ij} (\mathbf{R}_{ij} \mathbf{y}_j - \mathbf{y}_i),$$

i.e., each node adjusts its state such that the difference to its neighbors, after the characteristic transformation, is reduced, with information from all dimensions integrated. Summarising the states of all nodes into a vector $\mathbf{y} = (\mathbf{y}_1; \dots; \mathbf{y}_n)$, we have $\dot{\mathbf{y}} = -\mathcal{L}\mathbf{y}$.

The node state vectors then exhibit distinct behaviors in the multidimensional space, depending on the underlying MWN. If the network is coherent, multi-consensus can be achieved at the steady state, where nodes in different blocks are characterized by different vectors (see SM for more detail). In all other networks, the consensus dynamics will reach the steady state of all-zero vector for all nodes, i.e., global consensus, in a sufficiently long time, with the relaxation time depending on the level of coherence. We show later that the consensus dynamics on such networks can exhibit time-scale separation, where the states of nodes approach multi-consensus in a short time while converging to the all-zero state in the long run.

Random walks. Random walks is another important dynamics on networks, aiming at modeling how an entity randomly explores the underlying structure, with applications in various fields [38–45]. Now, let us consider a random walker that can not only randomly move on the network but change its states in its characteristic space \mathbb{R}^{n_d} . Specifically, for a random walker on node v_i at time t , it will choose one of v_i 's neighbors randomly at

$t + 1$, with probability w_{ij}/d_i for each neighbor v_j , while the characteristic vector will also transform according to the edge connecting them, through \mathbf{R}_{ij} . Hence, if we average the characteristic vectors at each node by the corresponding probability, denoted by \mathbf{y}_i for each node v_i , the (discrete-time) *random walks* on the network can be described as

$$\mathbf{y}_j(t+1) = \sum_i \frac{w_{ij}}{d_i} \mathbf{R}_{ij}^T \mathbf{y}_i(t) = \sum_i \frac{\mathbf{W}_{ij}^T \mathbf{y}_i(t)}{d_i}.$$

Furthermore, if we consider $\mathbf{y} = (\mathbf{y}_1; \dots; \mathbf{y}_n)$, then $\mathbf{y}(t+1) = \mathcal{P}^T \mathbf{y}(t) = (\mathcal{P}^T)^{t+1} \mathbf{y}(0)$, where \mathcal{P} is the supra-transition matrix.

With multidimensional interaction incorporated, the random walkers can explore the multidimensional sphere and exhibit averaged behavior that varies in accordance with the structure of MWN. If the network is coherent (and not bipartite), the averaged vector at the steady state will have different directions for nodes in different blocks (see SM for more detail). In all other networks, either there will be no steady state, or the averaged vector of each node will be all zero at steady state, i.e., there is no particular direction that is preferred by the random walkers. The relaxation time depends on the level of coherence.

Numerical results. We validate our theoretical results by using a matrix-weighted stochastic block model (MSBM). We generate a base network using a standard stochastic block model with n_b blocks, edge probability p_{in} within communities and p_{out} between communities ($p_{\text{in}} \geq p_{\text{out}}$). We first create a random base rotation matrix $\mathbf{R} \in \mathbb{R}^{n_d \times n_d}$ [46]. For nodes v_i and v_j in blocks k and ℓ respectively, we then set $\mathbf{R}_{ij} = \mathbf{R}^{\ell-k}$, ensuring coherence. To introduce variability, we perturb each \mathbf{R}_{ij} based on a disturbance parameter $\eta \in [0, 1]$ and a noise intensity $\sigma \geq 0$. With probability η , we apply additional random rotations with angles drawn from $\mathcal{N}(0, \sigma^2)$. We use 120 nodes divided into equal-sized communities. We test various configurations with dimensions $n_d \in \{2, 3, 5, 10\}$, edge probabilities $p_{\text{in}} = 0.3$ and $p_{\text{out}} \in \{0.1, 0.3\}$, number of communities $n_b \in \{2, 3, 4\}$, perturbation probabilities $\eta \in \{0, 0.2\}$, and noise intensities $\sigma^2 \in \{0, 0.1, 0.3\}$. All the configurations produced consistent results, and we report the representative results (see also SM).

The consensus dynamics on coherent MWNs align closely with our theoretical predictions (Fig. 3A–D). The node states converge towards their theoretical steady states, followed by a slow deviation within the distance of 10^{-13} . The incoherent case shows a distinct behavior: the state vectors first approach the steady state in the corresponding coherent case in a shorter time scale, followed by a notable deviation from the theoretical steady states (Figs. 3E–H). We observed the same behavior for different dimensions n_d and different numbers of communities n_b (see Robustness Analysis section in SM).

Notably, these dynamics for both coherent and incoherent cases remain consistent regardless of the presence ($p_{\text{in}} > p_{\text{out}}$) or absence ($p_{\text{in}} = p_{\text{out}}$) of topological community structure in the base network.

The random walk dynamics on MWNs align with our theoretical predictions (Fig. 4). We compare node states to their predicted steady states using angular distance rather than Euclidean distance, since they have the same direction instead of the exact states. We note that theoretical predictions focus on average behavior and are not normalized to the unit sphere, while individual node states in the coherent case are on the unit sphere. In coherent networks, node states converge angularly to their predicted steady states (Figs. 4A, B, D, and E). For incoherent networks, we observe a two-phase behavior. Initially, node states converge angularly to the steady state, followed by a stable deviation (Figs. 4G, H, J, K). The node states are drawn towards the origin (Figs. 4G, I, J, L), which occurs because node states are randomly mixed and averaged, smoothing out differences and resulting in a stable state at the origin.

Discussions. In this paper, we introduced a novel framework of MWNs, laying the mathematical groundwork for analyzing both their structural and dynamical properties. This approach opens new avenues for research in network science. For instance, random walks underpin numerous techniques for extracting insights from network data, such as determining node importance through centrality measures [47] and developing efficient community detection algorithms [6, 48]. Our framework provides an opportunity to extend these methods to datasets characterized by high-dimensional, interacting features. Our work also opens several fundamental questions for future research. In particular, we have explored in detail a strict notion of coherence in this paper but, as we discuss in SM, relaxed versions of coherence could be considered, leading to their own challenges.

This work participates in the recent efforts to enrich the standard network paradigm to “higher orders” [49]. MWNs could provide a new angle to analyze and generalize models of multilayer networks [12] and temporal networks [50], emphasizing the interaction between different dimensions (or layers). Take a system where each node is copied in n_d layers. Its connections via interlayer and intralayer connections to other nodes can be encoded in a matrix, making it possible to represent the system as a MWN. In addition, our definition of the matrix of a path, as the product of matrices of each of its edges, is a natural generalization of switching networks [51], a popular model for temporal networks, where the system is modeled as a random sequence of matrices, instead of a sequence determined by a walk on a graph as we consider here. In fact, any network with any node groupings can be modeled as an MWN, by defining the state of a node group as a vector and the interaction between groups as a matrix. We hope that MWNs not only deepen our un-

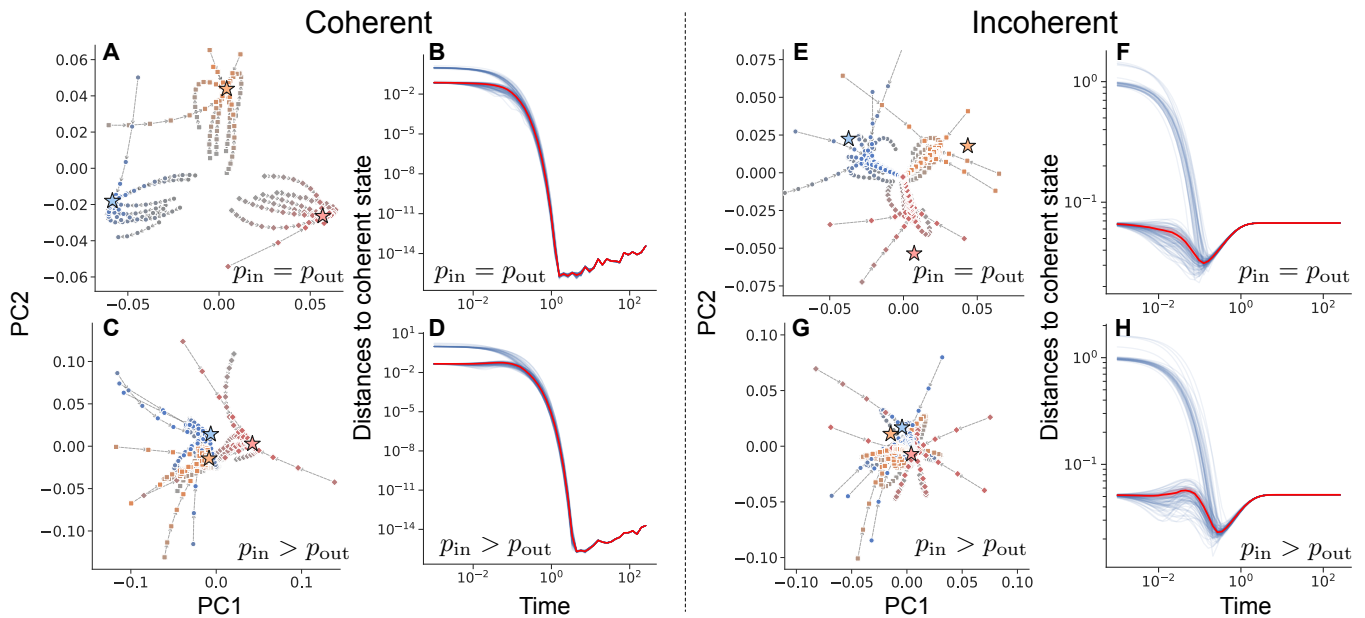


FIG. 3: Consensus dynamics in a three-block MSBM with 120 nodes and 10 dimensional state space. Red, yellow, and blue represent nodes in blocks 1, 2, and 3, respectively. Stars indicate theoretical steady states. We set $n_d = 10$, $p_{in} = 0.3$, $p_{out} = \{0.1, 0.3\}$. **A, B**: Coherent case, no topological community structure. **C, D**: Coherent case, strong topological community structure. **E, F**: Incoherent case, no topological community structure. **G, H**: Incoherent case, strong topological community structure. Panels A, C, E, G show PCA projections of state vector trajectories. In panels B, D, F, H, each blue line represents the distance to the steady state of a node, and the red line represents the average distance. The colorband indicates the 95% confidence interval estimated by 10^3 bootstrap sampling.

derstanding of complex systems but also provide a flexible framework for modeling a wide range of systems that have multidimensional dynamics at multiple scales.

Acknowledgments R.L. acknowledges support from the EPSRC grants EP/V013068/1, EP/V03474X/1 and EP/Y028872/1. Y.T. is funded by the Wallenberg Initiative on Networks and Quantum Information (WINQ).

[1] M. Newman, The empirical study of networks, in *Networks* (OUP Oxford, New York, 2018) 2nd ed., pp. 14–102.

[2] A. Jadbabaie, J. L., and A. Morse, Coordination of groups of mobile autonomous agents using nearest neighbor rules, *IEEE Trans. Automat. Control* **48**, 988 (2003).

[3] I. Couzin, J. Krause, N. Franks, and S. Levin, Effective leadership and decision-making in animal groups on the move, *Nature* **433**, 513 (2005).

[4] M. Porter and J. Gleeson, *Dynamical systems on networks: A tutorial*, Frontiers in Applied Dynamical Systems: Reviews and Tutorials (Springer, Heidelberg, Germany, 2016).

[5] R. Lambiotte and M. Schaub, *Modularity and Dynamics on Complex Networks*, Elements in Structure and Dynamics of Complex Networks (Cambridge University Press, 2022).

[6] M. Rosvall and C. Bergstrom, Maps of random walks

on complex networks reveal community structure, *PNAS* **105**, 1118 (2008).

[7] D. Cartwright and F. Harary, Structural balance: A generalization of heider’s theory, *Psychol. Rev.* **63**, 277 (1956).

[8] C. Altafini, Dynamics of opinion forming in structurally balanced social networks, *PLoS ONE* **7**, 1 (2012).

[9] Y. Tian and R. Lambiotte, Spreading and structural balance on signed networks, *SIAM J. Appl. Dyn. Syst.* **23**, 50 (2024).

[10] L. Böttcher and M. Porter, Complex networks with complex weights, *Phys. Rev. E* **109**, 024314 (2024).

[11] Y. Tian and R. Lambiotte, Structural balance and random walks on complex networks with complex weights, *SIAM J. Math. Data Sci.* **6**, 10.1137/23M158426 (2024).

[12] M. Kivela, A. Arenas, M. Barthelemy, J. Gleeson, Y. Moreno, and M. Porter, Multilayer networks, *J. Complex Netw.* **2**, 203 (2014).

[13] H. Sayama, Estimation of laplacian spectra of direct and strong product graphs, *Discrete Appl. Math.* **205**, 160 (2016).

[14] H. Sayama, Graph product multilayer networks: spectral properties and applications, *Journal of Complex Networks* **6**, 430 (2017).

[15] G. Bianconi, *Multilayer Networks: Structure and Function* (Oxford University Press, 2018).

[16] J. Schwinger, Unitary operator bases, *PNAS* **46**, 570 (1960).

[17] P. Barooah and J. Hespanha, Estimation from relative measurements: error bounds from electrical analogy, in

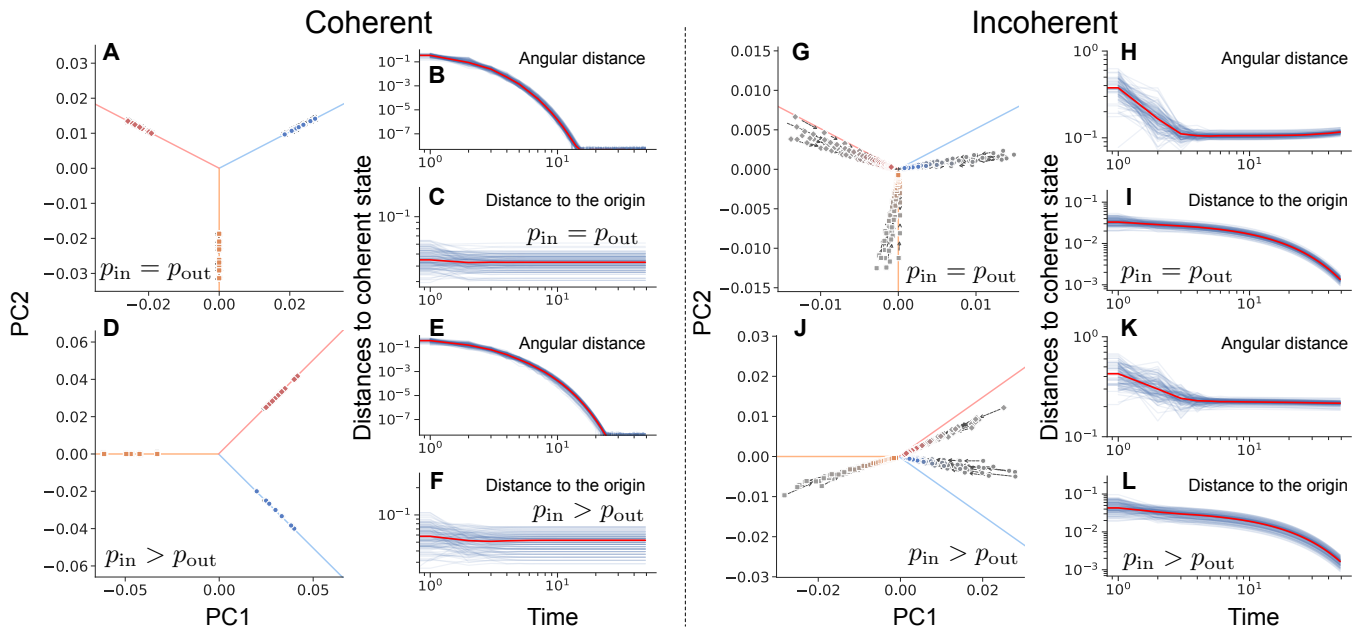


FIG. 4: Random walk dynamics in a three-block MSBM with 120 nodes and 10 dimensional state space. Red, yellow, and blue represent nodes in blocks 1, 2, and 3, respectively. The directions of the theoretical steady states are indicated by solid lines. We set $n_d = 10$, $p_{in} = 0.3$, $p_{out} = \{0.1, 0.3\}$. **A–C**: Coherent case, no topological community structure. **D–F**: Coherent case, strong topological community structure. **G–I**: Incoherent case, no topological community structure. **J–L**: Incoherent case, strong topological community structure. Panels A, D, G, J show PCA projections of state vector trajectories. Panels B, E, H, K show angular distances to steady state (blue: individual nodes, red: average). Panels C, F, I, L show distances to origin (blue: individual nodes, red: average). The colorband indicates the 95% confidence interval estimated by 10^3 bootstrap sampling.

Proceedings of 2005 International Conference on Intelligent Sensing and Information Processing, 2005. (2005) pp. 88–93.

- [18] A. Singer and H. Wu, Vector diffusion maps and the connection laplacian, *Communications on Pure and Applied Mathematics* **65**, 1067 (2012).
- [19] A. Novikov, D. Podoprikin, A. Osokin, and D. Vetrov, Tensorizing neural networks, in *Advances in Neural Information Processing Systems*, Vol. 28, edited by C. Cortes, N. Lawrence, D. Lee, M. Sugiyama, and R. Garnett (Curran Associates, Inc., 2015).
- [20] N. Friedkin, A. Proskurnikov, R. Tempo, and S. Parsegov, Network science on belief system dynamics under logic constraints, *Science* **354**, 321 (2016).
- [21] S. Parsegov, A. Proskurnikov, R. Tempo, and N. Friedkin, Novel multidimensional models of opinion dynamics in social networks, *IEEE Trans. Autom. Control* **62**, 2270 (2016).
- [22] M. Ye, J. Liu, L. Wang, B. Anderson, and M. Cao, Consensus and disagreement of heterogeneous belief systems in influence networks, *IEEE Trans. Autom. Control* **65**, 4679 (2019).
- [23] A. Nedić, A. Olshevsky, and C. Uribe, Graph-theoretic analysis of belief system dynamics under logic constraints, *Sci. Rep.* **9**, 8843 (2019).
- [24] M. Ye, M. Trinh, Y. Lim, B. Anderson, and H. Ahn, Continuous-time opinion dynamics on multiple interdependent topics, *Automatica* **115**, 108884 (2020).
- [25] H. Ahn, Q. Van Tran, M. Trinh, M. Ye, J. Liu, and K. Moore, Opinion dynamics with cross-coupling topics: Modeling and analysis, *IEEE Trans. Comput. Soc. Syst.* **7**, 632 (2020).
- [26] A. Bizyaeva, A. Franci, and N. E. Leonard, Multi-topic belief formation through bifurcations over signed social networks, arXiv preprint arXiv:2308.02755 (2023).
- [27] R. Axelrod, The dissemination of culture: A model with local convergence and global polarization, *J. Confl. Resolut.* **41**, 203 (1997).
- [28] J. Hansen and R. Ghrist, Opinion dynamics on discourse sheaves, *SIAM J. Appl. Math.* **81**, 2033 (2021).
- [29] C. Bodnar, F. Di Giovanni, B. Chamberlain, P. Lió, and M. Bronstein, Neural sheaf diffusion: A topological perspective on heterophily and oversmoothing in gnns, in *Advances in Neural Information Processing Systems*, Vol. 35 (Curran Associates, Inc., 2022) pp. 18527–18541.
- [30] L. Braithwaite, I. Duta, and P. Lió, Heterogeneous sheaf neural networks, arXiv preprint arXiv:2409.08036 (2024).
- [31] F. Barbero, C. Bodnar, H. de Ocariz Borde, M. Bronstein, P. Veličković, and P. Lió, Sheaf neural networks with connection laplacians, in *Proceedings of Topological, Algebraic and Geometric Learning Workshops 2022* (PMLR, 2022) pp. 28–36.
- [32] T. Gebhart, Graph convolutional networks from the perspective of sheaves and the neural tangent kernel, in *Proceedings of Topological, Algebraic and Geometric Learning Workshops 2022*, Proceedings of Machine Learning

Research, Vol. 196 (PMLR, 2022) pp. 124–132.

- [33] Code: Matrix-weighted networks for modeling multi-dimensional dynamics, <https://github.com/skojaku/matrix-weight-net> (2024), accessed: 2024-10-07.
- [34] N. Lynch, *Distributed Algorithms* (Morgan Kaufmann Publishers Inc., San Francisco, CA, USA, 1996).
- [35] T. Balch and L. Parker, *Robot Teams: From Diversity to Polymorphism*, 1st ed. (A K Peters/CRC Press, New York, NY, USA, 2002).
- [36] J. Russell Carpenter, Decentralized control of satellite formations, *Int. J. Robust Nonlin.* **12**, 141 (2002).
- [37] J. Fax and R. Murray, Information flow and cooperative control of vehicle formations, *IEEE Trans. on Autom. Control* **49**, 1465 (2004).
- [38] N. Masuda, M. Porter, and R. Lambiotte, Random walks and diffusion on networks, *Phys. Rep.* **716–717**, 1 (2017).
- [39] M. Fisher, Shape of a self-avoiding walk or polymer chain, *J. Chem. Phys.* **44**, 616 (1966).
- [40] G. Pinski and F. Narin, Citation influence for journal aggregates of scientific publications: Theory, with application to the literature of physics, *Info. Proc. Manag.* **12**, 297 (1976).
- [41] L. Page, S. Brin, R. Motwani, and T. Winograd, *The PageRank Citation Ranking: Bringing Order to the Web.*, Technical Report 1999-66 (Stanford InfoLab, 1999) previous number = SIDL-WP-1999-0120.
- [42] A. Okubo and S. Levin, *Diffusion and ecological problems: modern perspectives*, 2nd ed., Vol. 14 (Springer, New York, NY, USA, 2001).
- [43] W. Ewens, *Mathematical population genetics: theoretical introduction*, Vol. 27 (Springer, New York, NY, USA, 2004).
- [44] J. Gold and M. Shadlen, The neural basis of decision making, *Ann. Rev. Neurosc.* **30**, 535 (2007).
- [45] L. Gyllingberg, Y. Tian, and D. Sumpter, A minimal model of cognition based on oscillatory and reinforcement processes, arXiv preprint arXiv:2402.02520 [10.48550/arXiv.2402.02520](https://arxiv.org/abs/2402.02520) (2024).
- [46] We apply a series of random 2D rotations, for any pair of dimensions in a random order, to the identity matrix, with the angle drawn from a uniform distribution over $[-\pi, \pi]$.
- [47] D. Gleich, PageRank beyond the web, *SIAM Rev.* **57**, 321 (2015).
- [48] R. Lambiotte, J. Delvenne, and M. Barahona, Random walks, Markov processes and the multiscale modular organization of complex networks, *IEEE Trans. Netw. Sci. Eng.* **1**, 76 (2014).
- [49] R. Lambiotte, M. Rosvall, and I. Scholtes, From networks to optimal higher-order models of complex systems, *Nat. Phys.* **15**, 313 (2019).
- [50] P. Holme and J. Saramäki, Temporal networks, *Phys. Rep.* **519**, 97 (2012).
- [51] N. Masuda, K. Klemm, and V. Eguíluz, Temporal networks: slowing down diffusion by long lasting interactions, *Phys. Rev. Lett.* **111**, 188701 (2013).

SUPPLEMENTAL MATERIAL

Relaxed notion of coherence

At the core of the notion of coherence for matrix-weighted networks (MWNs), there is the condition that the transformation associated with any directed cycle C , e.g., starting at node v_i and composed of the edges $e_1, e_2 \dots, e_k$,

$$\mathbf{R}(C) = \mathbf{R}(e_1)\mathbf{R}(e_2)\dots\mathbf{R}(e_k),$$

is the identity matrix. Intuitively, the idea is that a signal, starting at node v_i , after it propagates along any cycle, will be mapped onto the same signal, solely from the transformations. This makes the existence of a non-trivial steady state possible. However, there could be situations where this condition is too strict.

One way to relax this condition would be to impose that only vectors along certain directions remain unchanged. We can consider the case when the matrix weights of all edges in C share the same eigenvector \mathbf{x} associated with eigenvalue 1 - a natural condition to ensure the conservation of a quantity along an edge. Then, coherence would be verified within this subspace spanned by \mathbf{x} , making it possible for non-trivial solutions for dynamical processes defined on MWNs. This definition of coherence could even be sufficient in the long time limit, in situations when 1 is the largest eigenvalue - this is the case for the transition matrix of random walks for instance -, and its corresponding eigenvector asymptotically dominates the dynamics. Alternative formulations could also consider cases when the shared eigenvector is not always associated with eigenvalue 1 but the product of such eigenvalues is 1 along C . We leave these questions for future research.

Additional mathematical results.

In this section, we give formal statements of the theoretical results presented in the paper and their detailed proofs.

Proposition 1. *The supra-Laplacian \mathcal{L} is positive semi-definite.*

Proof of Proposition 1. We write the supra-Laplacian matrix as a sum over the edges of G

$$\mathcal{L} = \sum_{(v_i, v_j), (v_j, v_i) \in E} \mathcal{L}^{\{i, j\}},$$

where $\mathcal{L}^{\{i, j\}} \in \mathbb{R}^{n_a \times n_a}$ also has block structure, and if we denote its k, l block as $\mathbf{L}_{kl}^{\{i, j\}} \in \mathbb{R}^{n_a \times n_a}$, the only

non-zero blocks are

$$\begin{aligned}\mathbf{L}_{ii}^{\{i,j\}} &= \mathbf{L}_{jj}^{\{i,j\}} = \|W_{ij}\|_2 \mathbf{I} = w_{ij} \mathbf{I} \\ \mathbf{L}_{ij}^{\{i,j\}} &= \mathbf{L}_{ji}^{\{i,j\}T} = -\mathbf{W}_{ij} = -w_{ij} \mathbf{R}_{ij}.\end{aligned}$$

For all $\mathbf{x} = (\mathbf{x}_1; \mathbf{x}_2; \dots; \mathbf{x}_n)$ with $\mathbf{x}_i \in \mathbb{R}^{n_d}$ for each i ,

$$\begin{aligned}\mathbf{x}^T \mathcal{L}^{\{i,j\}} \mathbf{x} &= \mathbf{x}_i^T w_{ij} \mathbf{x}_i + \mathbf{x}_j^T w_{ij} \mathbf{x}_j - \mathbf{x}_i^T w_{ij} \mathbf{R}_{ij} \mathbf{x}_j - \mathbf{x}_j^T w_{ij} \mathbf{R}_{ij}^T \mathbf{x}_i \\ &= w_{ij} (\mathbf{x}_i^T \mathbf{x}_i + \mathbf{x}_j^T \mathbf{x}_j - \mathbf{x}_i^T \mathbf{R}_{ij} \mathbf{x}_j - \mathbf{x}_j^T \mathbf{R}_{ij}^T \mathbf{x}_i) \\ &= w_{ij} (\mathbf{x}_i - \mathbf{R}_{ij} \mathbf{x}_j)^T (\mathbf{x}_i - \mathbf{R}_{ij} \mathbf{x}_j) \\ &= w_{ij} \|\mathbf{x}_i - \mathbf{R}_{ij} \mathbf{x}_j\|_2^2 \geq 0.\end{aligned}$$

Hence,

$$\mathbf{x}^T \mathcal{L} \mathbf{x} = \sum_{(v_i, v_j), (v_j, v_i) \in E} w_{ij} \|\mathbf{x}_i - \mathbf{R}_{ij} \mathbf{x}_j\|_2^2 \geq 0.$$

□

Definition 2. Let $G = (V, E, \mathcal{W})$ be a matrix-weighted graph. G is *coherent* if and only if the transformation of every directed cycle is \mathbf{I} .

Theorem 3 (structural theorem for balance). *A matrix-weighted graph G is coherent if and only if there is a partition $\{V_i\}_{i=1}^p$ s.t. (i) any edges within each node subset have transformation \mathbf{I} , (ii) any edges between the same pair of node subsets have the same transformation, and (iii) if we consider each node subset as a super node, then the transformation of any directed cycle is \mathbf{I} .*

Proof of Theorem 3. Suppose that such a partition exists. Then there are two possible cases for each directed cycle: it either completely lies in one of the node subset, thus has transformation \mathbf{I} , or contains one or more directed cycles by considering each node subset as a super node and edges within each node subset, thus the overall transformation is still \mathbf{I} . Hence, the graph is coherent by Definition 2.

Now suppose the graph is coherent. We first note that all matrix weights are then orthogonal matrices, i.e., $\mathbf{R}_{ij}^T = \mathbf{R}_{ij}^{-1}$ for all $(v_i, v_j) \in E$. We then construct the partition by applying the following rule to each node v_i : we group its neighbors together in the same node subset if the corresponding edges from v_i have the same transformation matrix, and we also group v_i to the node subset corresponding to transformation \mathbf{I} if there is any, and as a separate one otherwise (the ‘‘grouping rule’’) hereafter. We record the nodes to which the group rule has been applied after step k as \mathcal{V}_k and the resulting set of node subsets as \mathcal{P}_k , thus $\mathcal{V}_0 = \emptyset$ and $\mathcal{P}_0 = \emptyset$. We will show by induction that the group rule can be applied to all nodes without causing any conflict.

(i) When $k = 1$, it is trivial that applying the group rule does not cause conflict since $\mathcal{V}_0 = \emptyset$ and $\mathcal{P}_0 = \emptyset$.

(ii) Suppose that applying the grouping rule does not cause any conflict up to step $k - 1$. At step k , we select v_k as a neighbor of nodes in \mathcal{V}_{k-1} , and suppose by contradiction that applying the grouping rule to v_k will cause conflicts. Then there are four possibilities:

- 1) $\exists v_l \in \Gamma(v_k)$ s.t. v_l, v_k are in the same node subset in \mathcal{P}_{k-1} but $\mathbf{R}_{kl} \neq \mathbf{I}$;
- 2) $\exists v_l \in \Gamma(v_k)$ s.t. v_l, v_k are in a different node subsets in \mathcal{P}_{k-1} but $\mathbf{R}_{kl} = \mathbf{I}$;
- 3) $\exists v_l, v_m \in \Gamma(v_k)$ s.t. v_l, v_m are in the same node subset in \mathcal{P}_{k-1} , but $\mathbf{R}_{kl} \neq \mathbf{R}_{km}$;
- 4) $\exists v_l, v_m \in \Gamma(v_k)$ s.t. v_l, v_m are in the different node subsets in \mathcal{P}_{k-1} , but $\mathbf{R}_{kl} = \mathbf{R}_{km}$,

where $\Gamma(v_i) = \{v_j : (v_i, v_j) \in E\}$. In case 1), $v_l \notin \mathcal{V}_{k-1}$ since $\mathbf{R}_{kl} \neq \mathbf{I}$ and there is no conflict in \mathcal{P}_{k-1} . Then $\exists v_h \in \mathcal{V}_{k-1}$ s.t. $v_k, v_l \in \Gamma(v_h)$ and $\mathbf{R}_{hl} = \mathbf{R}_{hk}$. Hence, $\mathbf{R}_{hk} \mathbf{R}_{kl} \mathbf{R}_{lh} \neq \mathbf{I}$, which contradicts the graph being coherent. The contradiction in case 2) can be shown in a similar manner.

In case 3), since there is no conflict in \mathcal{P}_{k-1} , then either $(v_l, v_m) \in E$ with $\mathbf{R}_{lm} = \mathbf{I}$, or $\exists v_h \in \mathcal{V}_{k-1}$ s.t. $v_l, v_m \in \Gamma(v_h)$ and $\mathbf{R}_{hl} = \mathbf{R}_{hm}$. Then in the former, $\mathbf{R}_{kl} \mathbf{R}_{lm} \mathbf{R}_{mk} \neq \mathbf{I}$, while in the latter, $\mathbf{R}_{lh} \mathbf{R}_{hm} \mathbf{R}_{mk} \mathbf{R}_{kl} \neq \mathbf{I}$, both of which contradict the graph being coherent. The contradiction in case 4) can be shown in a similar manner. Hence, applying the grouping rule to v_k will not cause any conflict.

(iii) Finally, it is straightforward to check that the resulting partition has the features as stated. □

Theorem 4. *The supra-Laplacian matrix \mathcal{L} has eigenvalue 0 if and only if G is coherent. Furthermore, if \mathcal{L} has eigenvalue 0, the corresponding eigenvectors span the following subspace*

$$\mathbf{X} = \mathcal{S}^T (\mathbf{1} \otimes \mathbf{I}),$$

where \mathcal{S} is a block diagonal matrix that encodes the decomposition in Theorem 3. Specifically, let $\{V_i\}_{i=1}^p$ denote the corresponding partition, and \mathcal{S} has the i -th block on the diagonal being $\mathbf{S}_{1\sigma(i)}$, where $\sigma(\cdot)$ returns the node subset that a node is associated with, and \mathbf{S}_{hl} is the transformation of a directed path from nodes in V_h to V_l .

Proof of Theorem 4. \mathcal{L} has eigenvalue 0 if and only if there exists $\mathbf{x} = (\mathbf{x}_1; \mathbf{x}_2; \dots; \mathbf{x}_n)$ with $\mathbf{x}_i \in \mathbb{R}^{n_d}$ for each i , s.t.

$$\begin{aligned}\mathbf{x}^T \mathcal{L} \mathbf{x} &= \sum_{(i,j), (j,i) \in E} w_{ij} \|\mathbf{x}_i - \mathbf{R}_{ij} \mathbf{x}_j\|_2^2 = 0 \\ \Leftrightarrow \mathbf{x}_i &= \mathbf{R}_{ij} \mathbf{x}_j, \quad \forall (i, j) \in E.\end{aligned}\tag{2}$$

Condition (2) is true if and only if for any directed cycle in G , $C = \bigcup_{j=1}^l (v_{i_j}, v_{i_{j+1}})$ with the convention that $v_{i_{l+1}} =$

v_{i_1} , we have

$$\mathbf{R}_{i_1 i_2} \mathbf{R}_{i_2 i_3} \cdots \mathbf{R}_{i_i i_{i+1}} = \mathbf{I},$$

i.e., G is coherent.

In the case that 0 is an eigenvalue of \mathcal{L} , or G is coherent, from Theorem 3, we can write the supra-Laplacian matrix as

$$\mathcal{S}^T \bar{\mathcal{L}} \mathcal{S},$$

where \mathcal{S} is as defined in Theorem 4 and $\bar{\mathcal{L}}$ is the supra-Laplacian with identity matrix $\mathbf{I} \in \mathbb{R}^{n_d \times n_d}$ as the transformation of each edge,

$$\bar{\mathcal{L}} = \bar{\mathbf{L}} \otimes \mathbf{I},$$

where

$$\bar{\mathbf{L}} = \mathbf{D} - \bar{\mathbf{W}},$$

and $\bar{\mathbf{W}} = (w_{ij}) \in \mathbb{R}^{n \times n}$ only contains the magnitude information. We note that $\bar{\mathbf{L}}$ is the (ordinary) graph Laplacian corresponding to an undirected graph $\bar{G} = (V, \bar{E}, \bar{\mathbf{W}})$, thus 0 is an eigenvalue of $\bar{\mathbf{L}}$. Since \bar{G} is connected, there is only one eigenvector associated with 0, the all-one vector $\mathbf{1}$. The eigenvectors of \mathcal{L} associated with eigenvalue 0 can be obtained accordingly. \square

Proposition 5. *The supra-transition matrix \mathcal{P} has spectral radius no greater than 1, i.e., $\rho(\mathcal{P}) \leq 1$ where $\rho(\mathcal{P}) = \max\{|\lambda| : \lambda \text{ eigenvalue of } \mathcal{P}\}$. Furthermore, \mathcal{P} has eigenvalue 1 if and only if G is coherent, and has eigenvalue -1 if and only if $G_n = (V, E, -\mathcal{W})$, the graph obtained by negating each transformation matrix of each edge, is coherent.*

Proof. We know that $\mathcal{P} = \mathcal{I} - \mathcal{L}_{rw}$, and \mathcal{L}_{rw} is positive semi-definite from Proposition 1. Hence,

$$\lambda_{max}(\mathcal{P}) \leq 1,$$

where $\lambda_{max}(\cdot)$ returns the maximum eigenvalue of a matrix. Meanwhile, since $-\mathcal{P}$ is the supra-transition matrix of G_n ,

$$\lambda_{max}(-\mathcal{P}) \leq 1 \quad \Leftrightarrow \quad \lambda_{min}(\mathcal{P}) \geq -1,$$

where $\lambda_{min}(\cdot)$ returns the minimum eigenvalue of a matrix. Hence, we have

$$\rho(\mathcal{P}) \leq 1.$$

Specifically, \mathcal{P} has eigenvalue 1 if and only if 0 is an eigenvalue of \mathcal{L}_{rw} , if and only if G is coherent, from Theorem 4. The case of -1 being an eigenvalue of \mathcal{P} can be obtained in a similar way. \square

Proposition 6. *If G is coherent, then the consensus dy-*

namics will reach the steady state \mathbf{y}_j^ for each node v_j :*

$$\mathbf{y}_j^* = \mathbf{S}_{\sigma(j)1} \bar{\mathbf{y}}(0)/n$$

where $\bar{\mathbf{y}}(0) = \sum_{i=1}^n \mathbf{S}_{1\sigma(i)} \mathbf{y}_i(0)$, is the weighted average of the initial state vector with its characteristic transformation, $\{\mathbf{y}_i(0)\}$ is the set of initial state vectors, \mathbf{S}_{hl} and $\sigma(\cdot)$ are as defined in Theorem 4.

Proof of Proposition 6. From $\dot{\mathbf{y}} = -\mathcal{L}\mathbf{y}$, we can solve that

$$\mathbf{y}(t) = \exp(-\mathcal{L}t)\mathbf{y}(0)$$

where $\mathbf{y}(0) = (\mathbf{y}_1(0); \dots; \mathbf{y}_n(0))$ is the initial state vector. Since \mathcal{L} is symmetric, we can consider its unitary decomposition in terms of its eigenvalues $\lambda_1 \leq \dots \leq \lambda_{nn_d}$ and the associated orthonormal eigenvectors $\mathbf{x}_1, \dots, \mathbf{x}_{nn_d}$, respectively,

$$\mathcal{L} = \sum_{i=1}^{nn_d} \lambda_i \mathbf{x}_i \mathbf{x}_i^T.$$

Hence, we can write

$$\mathbf{y}(t) = \sum_{i=1}^{nn_d} \exp(-\lambda_i t) \mathbf{x}_i \mathbf{x}_i^T \mathbf{y}(0).$$

Then in the case that G is coherent,

$$\begin{aligned} \lim_{t \rightarrow \infty} \mathbf{y}(t) &= \sum_{i=1}^{n_d} \mathbf{x}_i \mathbf{x}_i^T \mathbf{y}(0) \\ &= (\mathcal{S}^T (\mathbf{1} \otimes \mathbf{I}) / \sqrt{n}) (\mathcal{S}^T (\mathbf{1} \otimes \mathbf{I}) / \sqrt{n})^T \mathbf{y}(0), \end{aligned}$$

where $\mathbf{x}_1, \dots, \mathbf{x}_{n_d}$ are the eigenvector associated with eigenvalue $\lambda_1 = \dots = \lambda_{n_d} = 0$, and the second equality is obtained from Theorem 4 and appropriate scaling for the eigenvectors to be orthonormal. Hence, the steady state \mathbf{y}_j^* for each node v_j can be obtained accordingly. \square

Proposition 7. *If G is coherent and is not bipartite, then the random walk will reach the steady state \mathbf{y}_j^* for each node v_j :*

$$\mathbf{y}_j^{*T} = \bar{\mathbf{y}}(0)^T \mathbf{S}_{1\sigma(j)} d_j / (2m)$$

where $\bar{\mathbf{y}}(0)^T = \sum_{i=1}^n \mathbf{y}_i(0)^T \mathbf{S}_{\sigma(i)1}$, is the weighted average of the initial characteristic vector with its characteristic transformation, $\{\mathbf{y}_i(0)\}$ is the set of initial characteristic vectors, $2m = \sum_j d_j$, \mathbf{S}_{hl} and $\sigma(\cdot)$ are as defined in Theorem 4.

Proof of Proposition 7. For random walks,

$$\mathbf{y}(t)^T = \mathbf{y}(0)^T \mathcal{P}^t.$$

Note that \mathcal{P} is not symmetric, but is similar to a symmetric matrix $\mathcal{P}_s = \mathcal{D}^{-1/2} \mathcal{W} \mathcal{D}^{-1/2}$, where $\mathcal{P} =$

$\mathcal{D}^{-1/2}\mathcal{P}_s\mathcal{D}^{1/2}$ thus for each eigenpair $(\lambda, \mathcal{D}^{1/2}\mathbf{x})$ of \mathcal{P}_s , (λ, \mathbf{x}) is a right eigenpair of \mathcal{P} . We denote the eigenvalues by $\lambda_1 \leq \dots \leq \lambda_{nn_d}$, with the associated eigenvectors of \mathcal{P} by $\mathbf{x}_1, \dots, \mathbf{x}_{nn_d}$, thus the eigenvectors of \mathcal{P}_s are $\mathcal{D}^{1/2}\mathbf{x}_1, \dots, \mathcal{D}^{1/2}\mathbf{x}_{nn_d}$. For illustrative purposes, we assume $\mathcal{D}^{1/2}\mathbf{x}_1, \dots, \mathcal{D}^{1/2}\mathbf{x}_{nn_d}$ to be orthonormal.

We know that $\mathcal{P}_s = \mathcal{I} - \mathcal{L}_{sys}$, where $\mathcal{L}_{sys} = \mathcal{D}^{-1/2}\mathcal{L}\mathcal{D}^{-1/2}$. Hence, \mathcal{L}_{sys} and \mathcal{P}_s share the same eigenvectors. Meanwhile, \mathbf{x} is an eigenvector of \mathcal{L} associated with eigenvalue 0 if and only if $\mathcal{D}^{1/2}\mathbf{x}$ is an eigenvector of \mathcal{L}_{sys} associated with 0. Hence, the eigenvectors of \mathcal{P}_s associated with 1 span the subspace,

$$\mathbf{X} = \mathcal{D}^{1/2}\mathcal{S}^T(\mathbf{1} \otimes \mathbf{I}),$$

where \mathcal{S} is a block diagonal matrix that encodes the decomposition in Theorem 3, from Theorem 4.

In the case that G is coherent and is not bipartite, 1 is an eigenvalue of \mathcal{P} but not -1 , from Proposition 5. Hence, we have

$$\begin{aligned} \lim_{t \rightarrow \infty} \mathcal{P}_s^t &= \lim_{t \rightarrow \infty} \sum_{i=1}^{nn_d} \lambda_i^t \left(\mathcal{D}^{1/2}\mathbf{x}_i \right) \left(\mathcal{D}^{1/2}\mathbf{x}_i \right)^T \\ &= \left(\mathcal{D}^{1/2}\mathcal{S}^T(\mathbf{1} \otimes \mathbf{I})/\sqrt{2m} \right) \left(\mathcal{D}^{1/2}\mathcal{S}^T(\mathbf{1} \otimes \mathbf{I})\sqrt{2m} \right)^T, \end{aligned}$$

where $2m = \sum_j d_j$. Hence,

$$\begin{aligned} \lim_{t \rightarrow \infty} \mathbf{y}(t)^T &= \lim_{t \rightarrow \infty} \mathbf{y}(0)^T \mathcal{P}^t = \lim_{t \rightarrow \infty} \mathbf{y}(0)^T \mathcal{D}^{-1/2} \mathcal{P}_s^t \mathcal{D}^{1/2} \\ &= \mathbf{y}(0)^T \mathcal{S}^T(\mathbf{1} \otimes \mathbf{I})/\sqrt{2m} \left(\mathcal{S}^T(\mathbf{1} \otimes \mathbf{I})\sqrt{2m} \right)^T \mathcal{D}. \end{aligned}$$

The steady state \mathbf{y}_j^* for each node v_j can be obtained accordingly. \square

Robustness Analysis

We observe that our results are consistently robust across different numbers of communities and dimensions of the state space (Figs. 5, 6, 7, and 8). The results demonstrate that the consensus dynamics for a three-block MSBM with 120 nodes in a 3-dimensional state space, and for a two-community MSBM with 120 nodes in a 3-dimensional state space align with our previous observations for three-block models in 10-dimensional space (Fig. 5 and 6). In all cases, we see similar patterns of convergence to steady states, with coherent cases showing convergence to the theoretical steady state and incoherent cases exhibiting initial convergence to the theoretical steady states followed by stable deviations. Similarly, for the random walk dynamics, the number of communities and the dimension of the state space do not affect the convergence patterns (Figs. 7 and 8). The impact of topological community structure on the dynamics is also consistent across these different configurations. This consistency across varying numbers of communities and state space dimensions underscores the robustness of our findings.

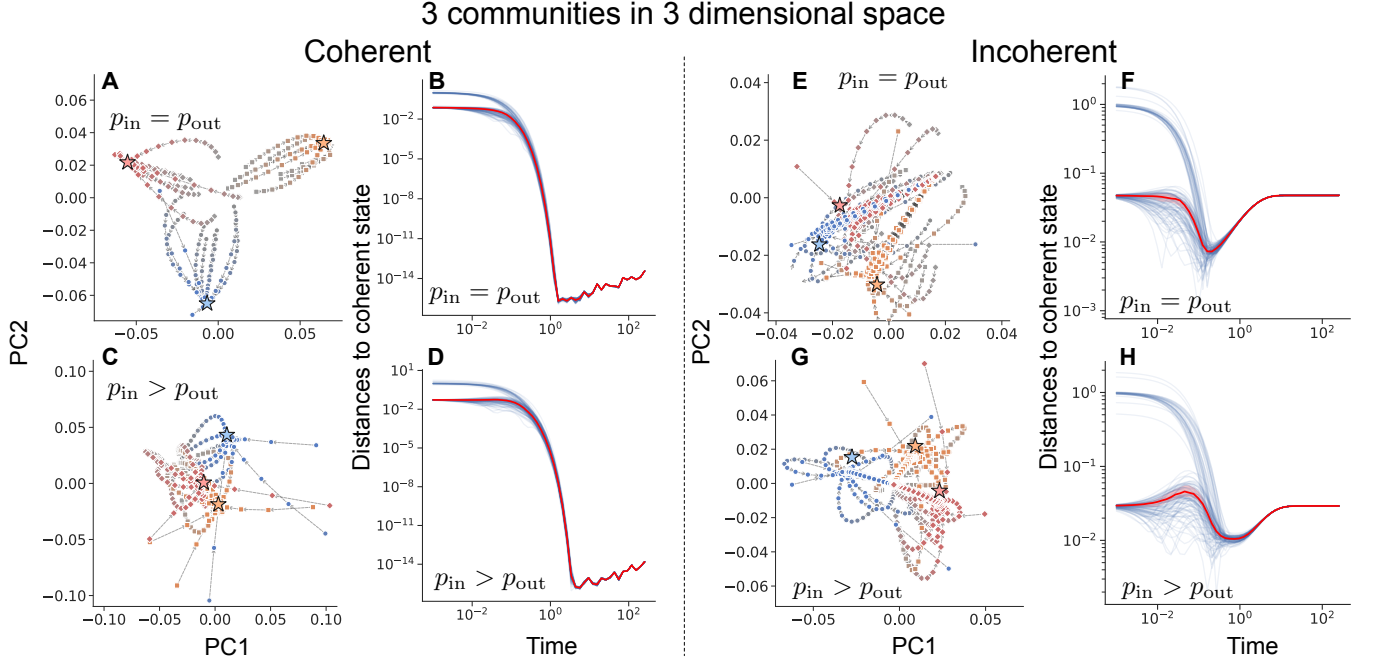


FIG. 5: Consensus dynamics in a three-block MSBM with 120 nodes and 3-dimensional state space. Red, yellow, and blue represent nodes in blocks 1, 2, and 3, respectively. The stars indicate the theoretical steady states. We set $n_d = 3$, $p_{\text{in}} = 0.3$, $p_{\text{out}} = \{0.1, 0.3\}$. **A–C**: Coherent case, no topological community structure. **D–F**: Coherent case, strong topological community structure. **G–I**: Incoherent case, no topological community structure. **J–L**: Incoherent case, strong topological community structure. Panels A, D, G, J show PCA projections of state vector trajectories. Panels B, E, H, K show distances to steady state (blue: individual nodes, red: average). Panels C, F, I, L show distances to origin (blue: individual nodes, red: average). The colorband indicates the 95% confidence interval estimated by 10^3 bootstrap sampling.

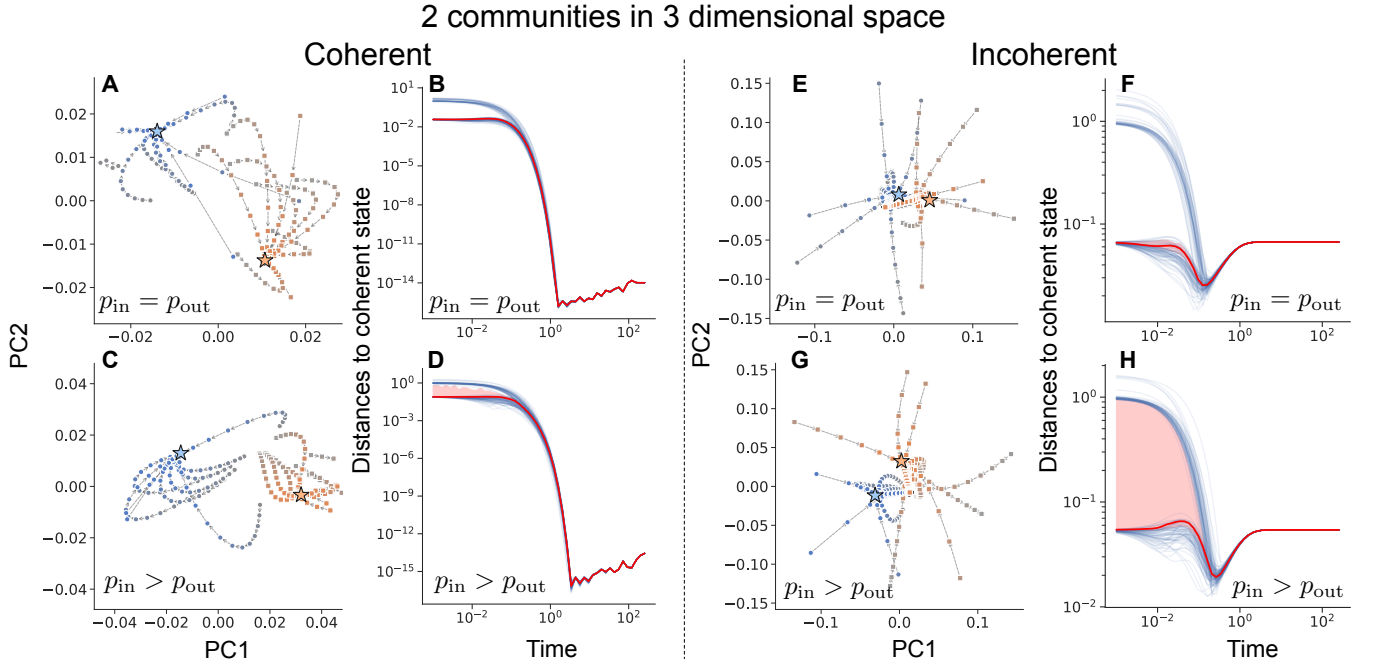


FIG. 6: Consensus dynamics in a three-block MSBM with 120 nodes of two communities and 3-dimensional state space. Yellow and blue represent nodes in blocks 1 and 2, respectively. The stars indicate the theoretical steady states. We set $n_d = 3$, $p_{\text{in}} = 0.3$, $p_{\text{out}} = \{0.1, 0.3\}$. **A–C**: Coherent case, no topological community structure. **D–F**: Coherent case, strong topological community structure. **G–I**: Incoherent case, no topological community structure. **J–L**: Incoherent case, strong topological community structure. Panels A, D, G, J show PCA projections of state vector trajectories. Panels B, E, H, K show distances to steady state (blue: individual nodes, red: average). Panels C, F, I, L show distances to origin (blue: individual nodes, red: average). The colorband indicates the 95% confidence interval estimated by 10^3 bootstrap sampling.

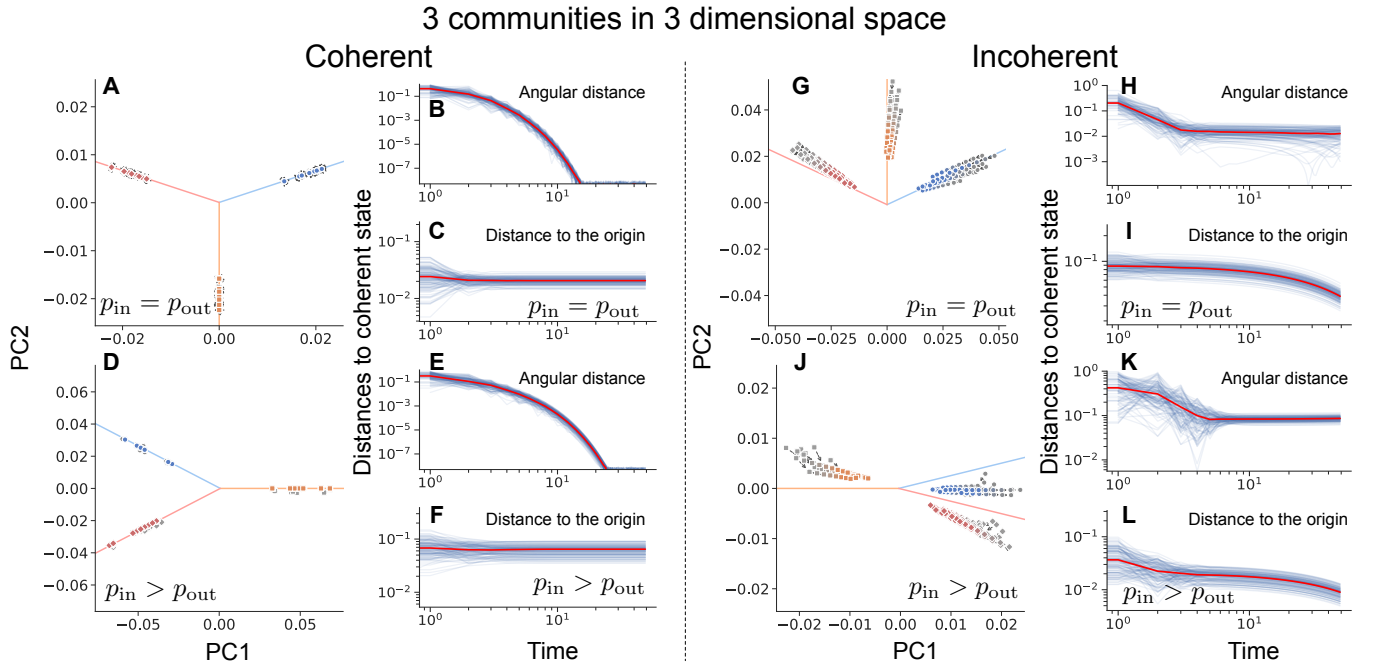


FIG. 7: Random walk dynamics in a three-block MSBM with 120 nodes and 3-dimensional state space. Red, yellow, and blue represent nodes in blocks 1, 2, and 3, respectively. The directions of the theoretical steady states are indicated by solid lines. We set $n_d = 3$, $p_{\text{in}} = 0.3$, $p_{\text{out}} = \{0.1, 0.3\}$. **A–C**: Coherent case, no topological community structure. **D–F**: Coherent case, strong topological community structure. **G–I**: Incoherent case, no topological community structure. **J–L**: Incoherent case, strong topological community structure. Panels A, D, G, J show PCA projections of state vector trajectories. Panels B, E, H, K show angular distances to steady state (blue: individual nodes, red: average). Panels C, F, I, L show distances to origin (blue: individual nodes, red: average). The colorband indicates the 95% confidence interval estimated by 10^3 bootstrap sampling.

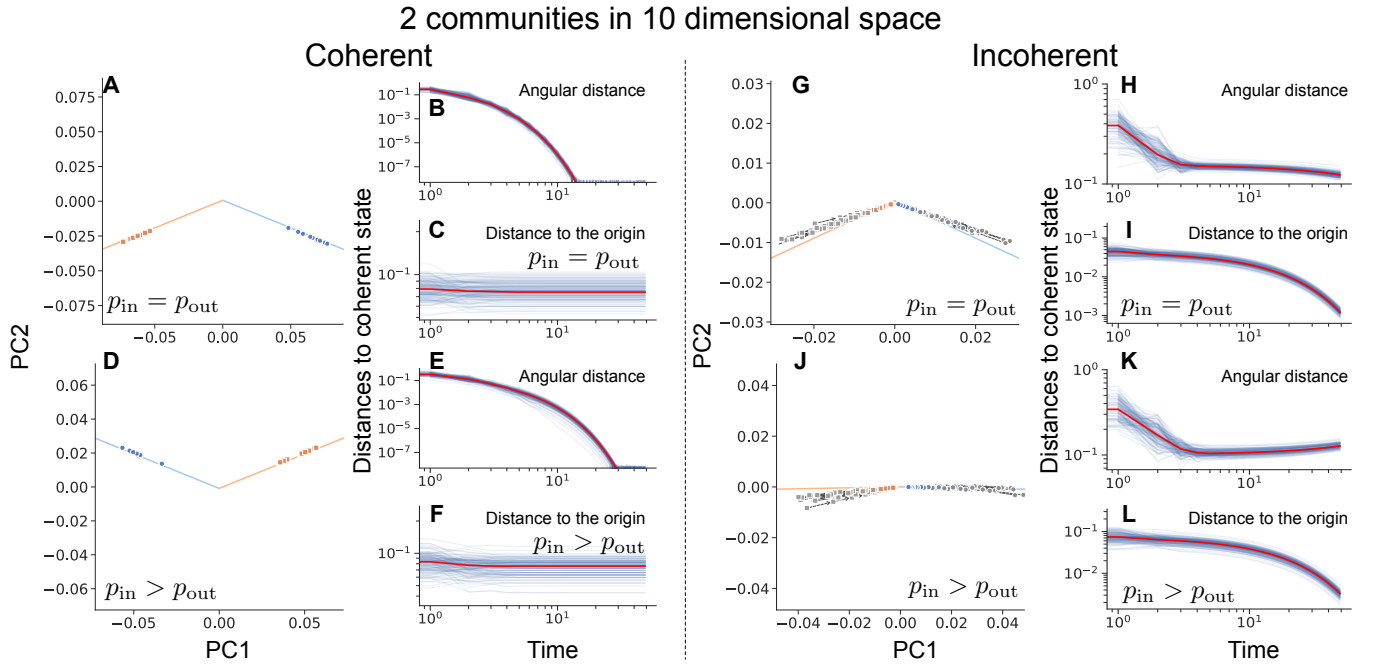


FIG. 8: Random walk dynamics in a three-block MSBM with 120 nodes of two communities and 10-dimensional state space. Yellow, and blue represent nodes in blocks 1 and 2, respectively. The directions of the theoretical steady states are indicated by solid lines. We set $n_d = 10$, $p_{in} = 0.3$, $p_{out} = \{0.1, 0.3\}$. **A–C**: Coherent case, no topological community structure. **D–F**: Coherent case, strong topological community structure. **G–I**: Incoherent case, no topological community structure. **J–L**: Incoherent case, strong topological community structure. Panels A, D, G, J show PCA projections of state vector trajectories. Panels B, E, H, K show angular distances to steady state (blue: individual nodes, red: average). Panels C, F, I, L show distances to origin (blue: individual nodes, red: average). The colorband indicates the 95% confidence interval estimated by 10^3 bootstrap sampling.